Environ Monit Assess (2019) 191:165
https://doi.org/10.1007/s10661-019-7251-4

Spatial and temporal distribution of metals in $PM_{2.5}$ during 2013: assessment of wind patterns to the impacts of geogenic and anthropogenic sources

Rodrigo Garza-Galindo · Ofelia Morton-Bermea · Elizabeth Hernández-Álvarez · Sara L. Ordoñez-Godínez · Omar Amador-Muñoz · Laura E. Beramendi-Orosco · Armando Retama · Javier Miranda · Irma Rosas-Pérez

Received: 25 May 2018 / Accepted: 21 January 2019

Abstract The Mexico City Metropolitan Area (MCMA) was the object of a chemical elemental characterization (Ti, V, Cr, Mn, Co, Ni, Cu, Mo, Ag, Cd, Sb, Pb, La, Sm, Ce, and Eu) of $PM_{2.5}$ collected during 2013 and analyzed by inductively coupled plasma mass spectrometry (ICP-MS). Sampling campaigns were carried out at five locations simultaneously—northwest, northeast, center, southwest, and southeast—during dry-warm season (April), rainy season (August), and dry-cold season (November). By means of enrichment factor (EF) and principal component analysis (PCA), it was possible to attribute the analyzed elements to geogenic and anthropogenic sources, as well as to identify a group of elements with mixed provenance sources. The highest concentrations for most metals were found in northwest and northeast, and during dry-warm (DW), confirming the trend observed in $PM_{2.5}$ samples collected in 2011. Despite similarities between 2011 and 2013, an increase of 17% in $PM_{2.5}$ mass concentration was observed, mainly attributable to geogenic sources, whereby the importance of wind intensity to the impact of emission sources is highlighted. The effect of wind intensity was revealed, by means of polar plots, as the controlling mechanism for this increase. This allowed us to conclude that high-speed episodes (5 m s^{-1}) were responsible for raising geogenic metal concentrations rather than wind direction.

Keywords $PM_{2.5}$ · Metals · Mexico City · Wind plots · Geogenic and anthropogenic sources

Electronic supplementary material The online version of this article (https://doi.org/10.1007/s10661-019-7251-4) contains supplementary material, which is available to authorized users.

R. Garza-Galindo
Posgrado en Ciencias de la Tierra, Universidad Nacional Autónoma de México, 04510 Mexico City, Mexico

O. Morton-Bermea (✉) · E. Hernández-Álvarez · S. L. Ordoñez-Godínez
Instituto de Geofísica, Universidad Nacional Autónoma de México, 04510 Mexico City, Mexico
e-mail: omorton@geofisica.unam.mx

O. Amador-Muñoz · I. Rosas-Pérez
Centro de Ciencias de la Atmósfera, Universidad Nacional Autónoma de México, 04510 Mexico City, Mexico

L. E. Beramendi-Orosco
Instituto de Geología and Labotarorio Nacional de Geoquímica y Mineralogía, Universidad Nacional Autónoma de México, 04510 Mexico City, Mexico

A. Retama
Secretaría del Medio Ambiente del Gobierno de la Cd. de México, 06000 Mexico City, Mexico

J. Miranda
Instituto de Física, Universidad Nacional Autónoma de México, 04510 Mexico City, Mexico

Introduction

The study of atmospheric particulate matter (PM) is relevant due to its toxic effects in humans and other living organisms as they are associated, according to the World Health Organization, to a broad spectrum of

Published online: 16 February 2019

acute and chronic illnesses, such as lung cancer, chronic obstructive pulmonary disease (COPD), and cardiovascular diseases (WHO 2016). Santibáñez-Andrade et al. 2017, Michael et al. 2013, and Kampa and Castanas 2008 have reported the relationship between long-term exposure of high concentrations of PM with increased risk of lung cancer and respiratory and cardiovascular diseases. Besides, transition metals present in PM are able to damage DNA, induce mutations, and initiate carcinogenesis (Perrone et al. 2013; Wang et al. 2016). In recent years, the elemental characterization of particulate matter with less than 2.5 μm of aerodynamic diameter ($PM_{2.5}$) has raised concern because this size represents the breathable fraction. Studies related to chemical characterization of metals in $PM_{2.5}$ in different areas of the world have increased both in urban and remote areas (Kulshrestha et al. 2009; Aldabe et al. 2011; Warneck and Williams 2012). Most of them discussed not only metal concentration levels but also their spatial distribution, concluding that these two features are mainly dominated from local factors at each given area (Dongarrà et al. 2010; Saliba et al. 2010; Moreno et al. 2011).

The need to identify and weigh the sources of metals in $PM_{2.5}$ has led to the combined application of sophisticated statistical tools to the chemical characterization of the data. In this way, natural and anthropogenic sources have been recognized (Alleman et al. 2010; Cheng et al. 2010). Natural emission sources include volcanic eruptions, mineral dust, and weathering of soils and rocks. The anthropogenic sources of metal emissions have been associated with punctual industrial activities, such as petrochemistry, manufacturing, smelting, mining, and mobile sources from vehicle transit.

However, the quantity of each single metal in $PM_{2.5}$ does not depend only on the magnitude of the source, but also on weather conditions; meteorological factors, such as wind direction and intensity, spread, dilute, or even accumulate metals in breathable air. The relationship between pollutant concentrations in the atmospheric environment and meteorological factors has been reported by Ledoux et al. (2017), Zhang et al. (2015), and Uria-Tellaetxe and Carslaw (2014). For instance, Zhang et al. 2015 report the cross-correlation between $PM_{2.5}$ concentration and meteorological factors. $PM_{2.5}$ concentration decrease when (1) temperature raises, which leads to diffusion and dilution of particulate matter due to frequency of air convection; (2) humidity raises, since particles will adsorb moisture and condensation will occur; and (3) wind speed raises, causing the spread of pollutants, which results in a lower concentration of $PM_{2.5}$, and vice versa. Conversely $PM_{2.5}$ increases by lower pressure, since this is not conducive to pollutant diffusion. Uria-Tellaetxe and Carslaw (2014) developed a new receptor modeling method (conditional bivariate probability function, CBPF) which requires wind speed as a variable to identify and characterize emission sources. Moreover, the same method was applied by Ledoux et al. 2016, finding the provenance of metals in $PM_{2.5}$ according to highest concentrations downwind as a first step for the identification of pollution sources related to their studied area. The Mexico City Metropolitan Area (MCMA) is one of the largest megacities in the world. It is located in a basin surrounded by mountains on the west, east, and south, with an average altitude of 2200 m above sea level. Only a few studies concerning atmospheric pollution have been conducted within the area; Megacity Initiative: Local and Global Research Observations (MILAGRO) campaign offers the results of several pollutant concentrations, such as CO, CO_2, SOx, NH_4^+, O_3 (DeCarlo et al. 2008; Querol et al. 2008; Stone et al. 2008; Mugica et al. 2009; Molina et al. 2010). In recent years, content and composition of organic compounds in PM have been reported by Amador-Muñoz et al. (2011, 2013), while metal content by particle-induced X-ray emission (PIXE) analysis has been reported by Miranda et al. (2005), Barrera et al. (2012), and Hernández-López et al. (2016) and Pt concentration by Morton-Bermea et al. (2014).

In a first stage of a research project to characterize the long-term variations in composition and temporal and spatial distribution of $PM_{2.5}$ in MCMA, we reported the seasonal and spatial behavior of elemental composition during 2011 (Morton-Bermea et al. 2018), highlighting the importance of local geogenic material and/or resuspension of soil dust, as the main source of metals to the $PM_{2.5}$ in the area, with anthropogenic sources having a minor contribution. Further, geogenic metal concentrations were consistent with the dominant wind direction from north to south. Despite the recognition of the importance of geogenic sources, further research was needed to confirm changes in the apportionment of such sources.

In this contribution, we aim to achieve a number of innovative goals relevant to the area first, to strengthen the $PM_{2.5}$ chemical database and link it to previous

results obtained with similar studies; second, to identify and assign metal enrichments to their geogenic and anthropogenic sources; and finally, to unravel the mechanism that causes shifts to the impact of these sources. This was accomplished by assessing metal concentrations to meteorological parameters, fundamentally wind patterns. The methodology implemented in this work is intended to become the basis for a monitoring program that would help to exhaustively understand the chemistry, meteorology, and temporal-spatial distribution of $PM_{2.5}$ in MCMA.

Methods

$PM_{2.5}$ sampling

Sampling of $PM_{2.5}$ was carried out in 2013 during three different seasons: dry-warm season (DW, April), rainy season (R, August), and dry-cold season (DC, November) at five sites simultaneously collected and located within MCMA: northwest (NW, Tlalnepantla), northeast (NE, San Agustín), central (C, Merced), southwest (SW, Coyoacán), and southeast (SE, Universidad Autónoma Metropolitana-Iztapalapa) (Fig. 1). The main features of the sampling sites are given in Table 1. $PM_{2.5}$ samples were collected for 24 h, every 6 days, on Teflon-impregnated glass fiber filter (20.4 cm × 25.2 cm; TIGF, Pallflex), previously baked at 280 °C. Samplings were carried out at $1.13 \pm 10\%$ m^3 min^{-1}, in high-volume samplers (Tisch and Andersen General Metal Works) previously calibrated according to Federal Register (1987). This sampling campaign belongs to a continuous program of environmental monitoring carried out by our research team employing infrastructure from the local government agency. In this way, 75 samples were collected for this study as well as for other researches. Unexposed filter for each sampling day was employed as field blank. Filters were enveloped in aluminum foil, kept in ziplock bags, and transported at 4 °C to the laboratory.

Sample treatment

$PM_{2.5}$ samples on filters were treated to analyze 16 elements (Ti, V, Cr, Mn, Co, Ni, Cu, Mo, Ag, Cd, Sb, Pb, La, Sm, Ce, and Eu). One-tenth of each filter was subjected to a microwave-assisted digestion procedure (Ethos One, Milestone) employing a mixture of aqua regia and HF. The digestion program was set from room temperature to 220 °C and kept for 20 min. The digested solution was taken to dryness and HNO_3 was added to ensure complete removal of HF. Finally, the digested solution was brought to 25-mL volume with 2% HNO_3 (*v*/*v*).

Instrumental analysis and quality control

Metal concentrations were obtained by means of inductively coupled plasma mass spectrometry (ICP-MS) in an iCAP Q spectrometer (Thermo Scientific) at Instituto de Geofísica, Universidad Nacional Autónoma de México. A multi-elemental calibration curve was performed including 0 ng mL^{-1}, 0.01 ng mL^{-1}, 0.1 ng mL^{-1}, 1 ng mL^{-1}, and 5 ng mL^{-1} concentration points as part of analytical controls. All standard solutions were prepared from a High Purity Standard (USA) solution with 2% HNO_3 (*v*/*v*) (Merck, Germany). Instrumental drift correction was made with ^{115}In as internal standard, prepared from a certified stock solution of 1000 mg L^{-1} (Merck, Germany).

Analytical quality was evaluated with the standard reference material SRM 1648a (urban particle matter) from NIST. Ten aliquots of SRM 1648a were prepared and analyzed in the same way as $PM_{2.5}$ samples. Blank test background contamination was monitored using operational blanks (unexposed filter papers), which were processed and analyzed with field samples. Detection limits were calculated as three times the standard deviation of 18 replicates of the procedural blank.

Data analysis

Mann-Whitney *U* test was used to compare medians among seasons and sites. The significant difference was defined as $p < 0.05$. Spearman's correlation was used to evaluate association among variables. Principal component analysis (PCA) with Spearman's correlation matrix and varimax rotation algorithm was used to identify sources. Statistica Software V 10.0 (StatSoft, USA) was used for the statistical analyses. Metal enrichment factors (EF) were computed based on metal crust data from Wedepohl (1995).

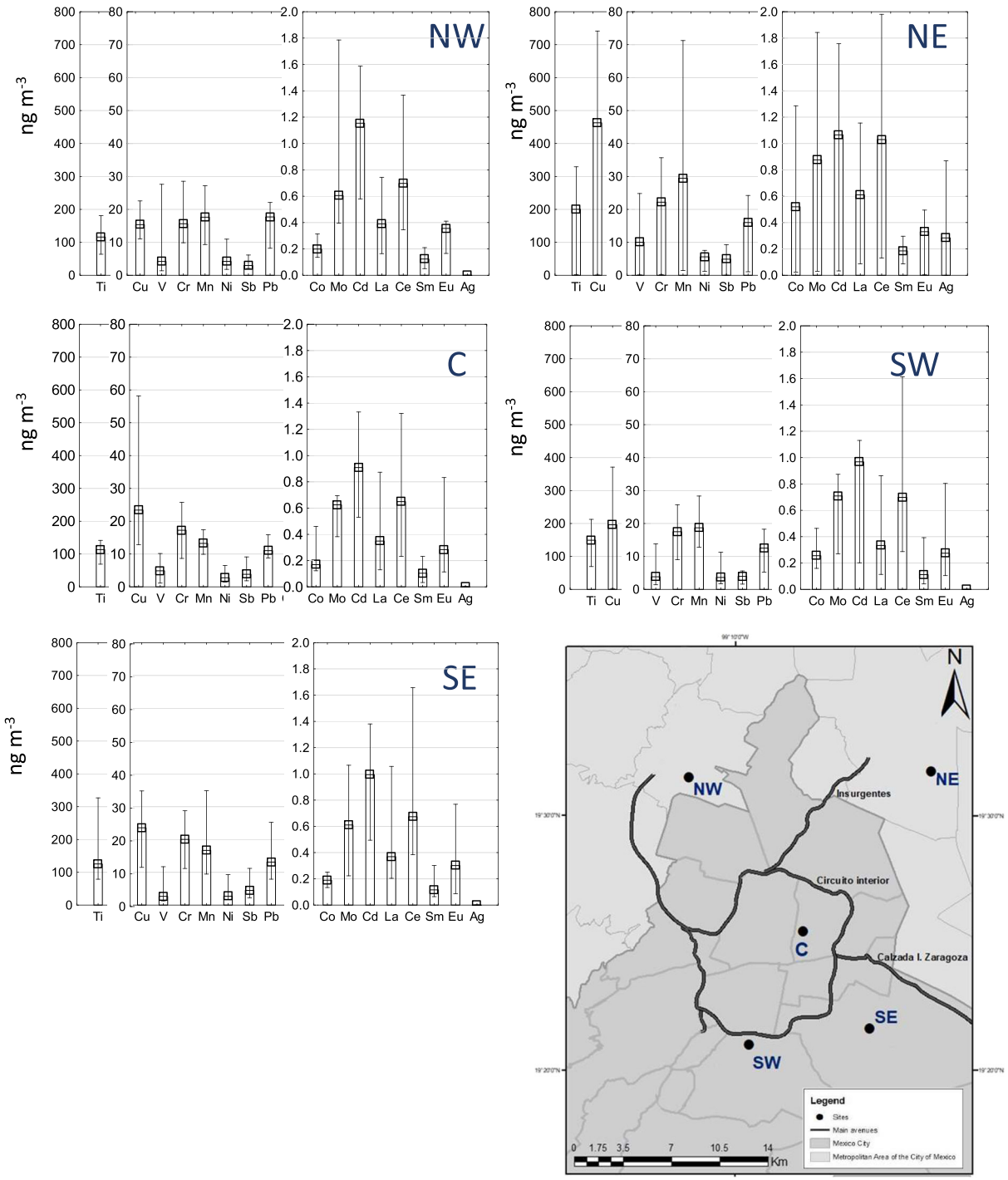

Fig. 1 Spatial distribution for the 16 metals analyzed in $PM_{2.5}$

Meteorological data

Meteorological parameters comprising temperature (*T*), relativity humidity (RH), wind speed (Wsp), and wind flow (Wfl), along with $PM_{2.5}$ mass concentration, were obtained from the local air quality monitoring authority SEDEMA (available online database at: http://www.aire.df.gob.mx/default.php?opc=%27aKBhnmI=%27&opcion=Zw).

Table 1 Sampling site characteristics

Site name	Position in MCMA	Main characteristics
Tlalnepantla	Northwest, NW	Residential and commercial area with industrial settlement and traffic avenues
San Agustín	Northeast, NE	Residential and commercial area with few industrial settlement and avenues
Merced	Central, C	Commercial and residential zone with vehicular avenues
Coyoacán	Southwest, SW	Residential zone and vehicular avenue
Universidad Autónoma Metropolitana-Iztapalapa	Southeast, SE	Residential zone and vehicular avenue with small manufactories

Results and discussion

Quality control

Metal recoveries and relative standard deviation (RSD) are given in Table 2. Recoveries ranged from 60 to 102%. Mo and Eu are not included as certified elements in SRM1648a; however, they were considered in this study because the analytical method resulted in RSD between 0.86 and 1.1%, $n = 18$. The accurate recovery rates are comparable to other reported ICP-MS analytical procedures, including microwave-assisted digestion and different mixtures of acids and SRM (Dongarrà et al. 2010; Aldabe et al. 2011; Hays et al. 2011; Morton-Bermea et al. 2018).

Relationship between $PM_{2.5}$ mass concentration and meteorological parameters

Seasonal $PM_{2.5}$ concentrations and meteorological parameters are tabulated in Table 3. The annual median $PM_{2.5}$ mass concentration found for the sampling period is 28 μg $m^{-3} \pm 15$ μg m^{-3}. This value exceeds two times the local recommended limit (12 μg m^{-3}, NOM-025-SSA1-2014) and almost three times the international recommendation (10 μg m^{-3}, WHO 2005). The Mann-Whitney *U* test shows that the highest mass concentration was registered during DW (38 μg m^{-3}, $p < 0.05$) by lowest RH and Wsp ($p < 0.05$) (Table 3). These observations agree with the conditions imposed by the low RH and Wsp that does not favor the dispersion of PM, as well observed by Zhang et al. 2015.

Elemental composition of $PM_{2.5}$: spatial and seasonal behavior

Metal concentrations in $PM_{2.5}$ are listed in Table 4. Titanium was the most abundant metal with more than 50% relative abundance and Cu represents 13%, while Mn, V, Cr, Pb, Ni, and Sb sum for 27%; metals such as Mo, Cd, La, Sm, Eu, and Ce computed for less than 0.1% each. The spatial metal behavior is depicted in Fig. 1 with metal median concentrations at the five sites during the sampling season. The spatial comparison via Mann-Whitney *U* test (reported in Table S1) shows no significant differences for Cr, V, and Sb; this can be interpreted as the result of homogenization processes, or of a similar impact of the same source within the study area. On the other hand, Cd, Ni, and Pb present a significant difference at NE and NW. The remaining analyzed metals (Ti, Mn, Co, Cu, Mo, and Ag) have significant differences among the regions of MCMA, with concentrations in the following order: NE > NW > SW = C = SE. These findings align with those previously reported in Morton-Bermea et al. 2018. The contribution of this study, obtained from a more in-depth analysis ("Source apportionment" and "Relationship between metal concentration and wind patterns" sections) of the effects of winds on the dispersion allowed us to weigh the sources responsible for the high concentrations of metals observed in the north sites (NW and NE). The attribution of the enrichment of metals in the north of the studied area is complicated because of an industrial settlement and its proximity to arid areas further north of MCMA which Morton-Bermea et al. 2018 identify as a source of geogenic contamination in the studied area.

Table 2 Metal recoveries from SRM1648a

Analyte	NIST 1648a (mg kg^{-1})	Experimental (mg kg^{-1})	% Recovery	RSD	Detection limit (mg kg^{-1})
Ti	4021	4107	102.1	9.8	2.40
V	127	105	83.2	7.3	0.25
Cr	402	335	83.4	8.2	0.24
Mn	790	667	84.5	5.8	0.43
Co	17.93	12.68	70.8	5.1	0.02
Ni	81.1	66.73	82.3	5.2	0.36
Cu	610	379	62.1	8.7	1.10
Ag	6.0	3.5	59.1	9.6	0.07
Cd	73.7	64.1	86.9	4.1	0.25
Sb	45.4	36.4	81.1	7.8	0.11
Pb	0.655	0.48	73.3	7.0	0.25
La	39	27.8	71.3	9.8	0.07
Ce	54.6	35.6	65.2	9.3	0.90
Sm	4.3	2.8	65.1	9.5	0.23

$n = 18$. Al, Fe, and Zn could not be satisfactorily recovered

RSD relative standard deviation

A comparison by means of a *U* test for the seasonal data (Table S2) shows two behaviors: Cu, Cr Ni, V, Cd, and Mo with concentrations increasing in the following order R < DW < DC and Ti, Mn, Co, Sb, and Pb present no seasonal significant variation. This behavior can derive mainly from two phenomena: (1) variations in the magnitude of the sources of these metals and (2) atmospheric processes of dispersion and accumulation.

Table 5 and Table 6 compare data obtained in this study with data obtained for $PM_{2.5}$ collected during 2011 using the same sampling protocol (Morton-Bermea et al. 2018). There was an increase in $PM_{2.5}$ mass concentration during 2013 of up to 17% as compared to that during 2011 ($p < 0.05$). According to this, an increase of metal concentrations could be expected; nonetheless, this is only true for metals identified as geogenic (Morton-Bermea et al. 2018). Ti, Mn, Sm, Eu, and Ce were increased by 30%. Conversely, concentration of metals commonly considered from anthropogenic origin decreased: Cd and Sb both reduced in 18%, Pb in 37% and Ni and V in 30% and 56%, respectively. Spatial trends showed similar behavior in 2011 and 2013, except for the SW sampling site, where metal concentrations in general decreased from 2011 to 2013. Assuming small changes in emission sources for this period, these changes could be attributed to

Table 3 Meteorological parameters for MCMA during 2013 sampling campaign. Significant differences ($p < 0.05$) are indicated in **bold** when values are the highest among seasons, and values are ***bold italics*** when values are significantly the lowest, analysis by Mann-Whitney *U* test

	2013			DW ($n = 25$)			R ($n = 25$)		DC ($n = 25$)				*U* test trend
	X	*M*	SD	*X*	*M*	SD	*X*	*M*	SD	*X*	*M*	SD	
$PM_{2.5}$ (μg m^{-3})	28.1	24.5	15.1	40.0	**38.0**	17.4	17.9	***16.0***	11.1	31.5	25.0	23.3	DW > DC > R
T (°C)	17.0	16.9	3.7	21.1	**21.3**	4.6	17.1	16.1	3.7	14.4	***13.9***	4.3	DW > R > DC
RH	52.6	57.5	21.4	28.9	***25.0***	16.5	65.0	**68.0**	19.7	61.5	65.0	18.4	R > DC > DW
Wsp (m s^{-1})	2.2	2.1	0.5	2.2	***1.8***	1.2	2.3	**2.2**	1.0	2.1	1.9	0.9	R > DC = DW

T temperature, RH relative humidity, *Wsp* wind speed, *X* mean, *M* median, SD standard deviation, *DW* dry-warm, *R* rainy, *DC* dry-cold

Table 4 Statistical data of metal concentrations found in $PM_{2.5}$

Metal	Median (ng m^{-3})	Mean (ng m^{-3})	SD (ng m^{-3})	Min (ng m^{-3})	Max (ng m^{-3})	% RSD	Relative abundance (%)
Ti	139	227	466	2.08	3862	205	57
V	4.6	29	93	0.09	761	322	2
Cr	18	25	31	0.19	217	122	8
Mn	18	32	69	1.46	567	213	7
Co	0.24	0.55	1.7	0.02	15	307	0.1
Ni	3.6	7.9	15.7	1.21	114	199	1.5
Cu	31	213	614	0.64	5181	289	13
Mo	0.66	1.02	1.61	0.03	12	158	0.3
Cd	0.99	1.33	1.74	0.03	13	131	0.4
Sb	4.0	5.6	8	0.03	54	142	2
Pb	13	17	17	1.07	125	102	5
Ag	0.01	0.10	0.31	0.0	2.8	310	< 0.1
La	0.40	0.70	1	0.1	7.8	143	< 0.1
Sm	0.10	0.20	0.3	0.0	1.9	150	< 0.1
Eu	0.30	0.50	0.8	0.0	6.5	160	< 0.1
Ce	0.70	1.20	1.7	0.1	10	142	< 0.1

SD standard deviation, *CV* coefficient variation, *RSD* relative standard deviation

Table 5 Comparison of $PM_{2.5}$ and meteorological parameters between 2011 and 2013

	2011[a]				2013			
	N	Mean	Median	SD	*N*	Mean	Median	SD
$PM_{2.5}$ (μg m^{-3})	78	21.7	21.0	9.1	74	**28.1**	**24.5**	15.1
T (°C)	62	17.6	17.6	2.9	68	17.0	16.9	3.7
RH	69	50.7	57.5	17.7	67	52.6	57.5	21.4
Wsp (ms^{-1})	74	2.2	2.2	0.6	65	2.2	2.1	0.5
	DW 2011[a]				DW 2013			
$PM_{2.5}$ (μg m^{-3})	25	29.8	31.0	6.5	25	**39.4**	**41.5**	10.6
T (°C)	18	20.6	20.9	1.9	24	21.1	20.8	1.9
RH	20	**44.8**	**45.8**	**16.7**	24	28.4	24.5	12.2
Wsp (ms^{-1})	20	1.8	1.7	0.3	25	2.2	2.1	0.5
	R 2011[a]				R 2013			
$PM_{2.5}$ (μg m^{-3})	28	13.3	13.5	5.0	24	16.2	14.3	6.6
T (°C)	29	**17.6**	**17.6**	**1.2**	20	16.2	16.3	1.8
RH	24	54.4	59.8	18.5	20	**67.5**	**61.5**	13.1
Wsp (ms^{-1})	29	2.5	2.4	0.4	20	2.3	2.2	0.5
	DC 2011[a]				DC 2013			
$PM_{2.5}$ (μg m^{-3})	25	22.9	23.5	6.5	25	**28.4**	**24.0**	16.4
T (°C)	15	**14.2**	**14.5**	**2.2**	24	13.6	13.1	2.0
RH	25	52.0	60.0	17.2	23	**64.9**	**66.5**	8.7
Wsp (ms^{-1})	25	2.1	1.7	0.6	20	2.1	1.9	0.6

Values marked in bold are significant higher ($p<0.05$)

[a] Data from Morton-Bermea et al. (2018)

Table 6 Comparison of metal concentrations found in this study and those coincident from the 2011 campaign (Morton-Bermea et al. 2018)

Metal	Mean ng m^{-3} 2011[a]	Median ng m^{-3}	SD ng m^{-3}	Mean ng m^{-3} 2013	Median ng m^{-3}	SD ng m^{-3}	Mean ng m^{-3} DW 2011[a]	Median ng m^{-3}	SD ng m^{-3}	Mean ng m^{-3} DW 2013	Median ng m^{-3}	SD ng m^{-3}
Ti	115.4	107.6	58.4	**227.0**	**138.8**	**466.3**	146.6	130.6	70.5	197.2	125.3	217.5
V	**15.0**	**10.4**	**15.2**	28.8	4.6	92.6	**10.6**	**11.0**	**4.1**	37.5	6.1	150.8
Cr	18.1	18.0	6.4	25.4	18.4	31.0	**21.3**	**22.2**	**6.3**	21.7	16.0	30.1
Mn	15.7	13.6	9.4	**32.3**	**17.6**	**68.7**	17.1	13.8	11.0	27.6	16.7	28.6
Co	0.3	0.2	0.3	0.5	0.2	1.7	0.4	0.3	0.3	0.4	0.2	0.5
Ni	**6.0**	**5.2**	**3.6**	7.9	3.6	15.7	**7.1**	**7.6**	**3.1**	8.2	3.6	22.0
Cu	60.2	28.3	72.4	212.6	30.5	614.3	49.5	26.0	50.2	**168.3**	**65.5**	**184.6**
Cd	**1.2**	**1.2**	**0.5**	1.3	1.0	1.7	1.1	0.9	0.7	1.7	1.1	2.4
Sb	**5.5**	**4.8**	**3.3**	5.6	3.9	8.0	5.2	5.1	2.2	7.4	4.9	10.0
Pb	**25.1**	**20.8**	**14.3**	16.9	13.1	17.3	**25.1**	**20.5**	**15.4**	17.2	11.7	19.3
La	0.72	0.46	0.63	0.66	0.40	1.02	**1.31**	**1.23**	0.82	0.62	0.33	1.50
Sm	0.18	0.11	0.16	0.21	0.14	0.25	**0.33**	**0.32**	0.20	0.18	0.11	0.36
Eu	0.22	0.20	0.13	**0.49**	**0.32**	0.78	0.20	0.13	0.14	**0.49**	0.11	1.25
	R 2011[a]			R 2013			DC 2011[a]			DC 2013		
Ti	112.2	106.8	35.7	183.7	123.8	245.4	89.4	75.0	56.2	**300.1**	**148.0**	**744.6**
V	**10.3**	**6.2**	**9.3**	4.7	2.5	5.3	24.9	20.9	22.1	44.2	19.3	52.6
Cr	19.7	19.0	4.2	28.2	20.0	39.7	13.1	11.5	5.8	**26.2**	**23.2**	**21.4**
Mn	16.8	14.9	6.7	26.6	18.0	39.0	12.9	9.1	10.2	**42.7**	**20.6**	**109.7**
Co	0.3	0.2	0.3	0.3	0.2	0.5	0.3	0.2	0.2	**0.9**	**0.3**	**2.9**
Ni	**5.0**	**4.9**	**3.1**	4.3	3.3	4.0	6.2	6.3	4.5	11.3	5.6	15.3
Cu	63.8	31.9	73.6	339.6	25.0	1028.1	66.2	23.2	88.9	129.9	21.0	215.9
Cd	**1.5**	**1.5**	**0.4**	1.1	0.8	1.6	1.0	1.0	0.4	1.1	1.1	0.8
Sb	**5.2**	**4.9**	**2.0**	4.9	2.8	9.2	6.1	4.3	5.1	4.5	3.9	2.6
Pb	**29.9**	**27.9**	**13.8**	18.9	13.5	22.4	19.1	17.4	11.8	14.7	14.3	5.8
La	0.51	0.40	0.30	0.65	0.53	0.56	0.40	0.38	0.22	**0.70**	**0.61**	**0.80**
Sm	0.15	0.13	0.08	0.23	0.18	0.19	0.08	0.08	0.06	**0.21**	**0.17**	**0.18**
Eu	0.28	0.25	0.14	**0.52**	**0.35**	**0.42**	0.19	0.20	0.09	**0.47**	**0.35**	**0.34**

Values marked in bold are significant higher ($p<0.05$)

SD standard deviation

[a] Data from Morton-Bermea et al. (2018)

Table 7 Spearman correlation rank. Significant values ($p < 0.05$) are marked in **bold**

	$PM_{2.5}$	Ti	V	Cr	Mn	Co	Ni	Cu	Mo	Cd	Sb	La	Ce	Sm	Eu	Pb	Ag
$PM_{2.5}$	1.000	0.082	**0.649**	−0.170	0.119	0.184	**0.371**	0.165	**0.290**	**0.351**	**0.641**	−0.059	−0.141	−0.164	0.073	0.018	−0.017
Ti	0.082	1.000	**0.335**	**0.730**	**0.938**	**0.811**	**0.374**	**0.473**	**0.554**	0.092	**0.362**	**0.588**	**0.722**	**0.670**	**0.391**	**0.417**	**0.493**
V	**0.649**	**0.335**	1.000	0.194	**0.419**	**0.491**	**0.722**	**0.255**	**0.708**	**0.420**	**0.619**	**0.277**	0.196	0.175	**0.249**	**0.338**	**0.339**
Cr	−0.170	**0.730**	0.194	1.000	**0.663**	**0.458**	**0.326**	0.198	**0.452**	0.023	0.101	**0.707**	**0.736**	**0.774**	**0.605**	**0.444**	**0.305**
Mn	0.119	**0.938**	**0.419**	**0.663**	1.000	**0.862**	**0.457**	**0.477**	**0.648**	0.193	**0.351**	**0.585**	**0.686**	**0.624**	**0.385**	**0.528**	**0.466**
Co	0.184	**0.811**	**0.491**	**0.458**	**0.862**	1.000	**0.525**	**0.544**	**0.685**	**0.244**	**0.410**	**0.512**	**0.587**	**0.504**	**0.302**	**0.478**	**0.483**
Ni	**0.371**	**0.374**	**0.722**	**0.326**	**0.457**	**0.525**	1.000	0.213	**0.571**	**0.274**	**0.331**	**0.464**	**0.386**	**0.388**	**0.451**	**0.544**	**0.350**
Cu	0.165	**0.473**	**0.255**	0.198	**0.477**	**0.544**	0.213	1.000	**0.316**	0.099	**0.466**	**0.229**	**0.264**	0.161	−0.019	**0.279**	**0.459**
Mo	**0.290**	**0.554**	**0.708**	**0.452**	**0.648**	**0.685**	**0.571**	**0.316**	1.000	**0.443**	**0.506**	**0.425**	**0.408**	**0.376**	**0.312**	**0.473**	**0.529**
Cd	**0.351**	0.092	**0.420**	0.023	0.193	**0.244**	**0.274**	0.099	**0.443**	1.000	**0.631**	−0.091	−0.124	−0.141	−0.035	**0.501**	0.140
Sb	**0.641**	**0.362**	**0.619**	0.101	**0.351**	**0.410**	**0.331**	**0.466**	**0.506**	**0.631**	1.000	0.100	0.095	0.040	0.094	**0.365**	**0.301**
La	−0.059	**0.588**	**0.277**	**0.707**	**0.585**	**0.512**	**0.464**	**0.229**	**0.425**	−0.091	0.100	1.000	**0.929**	**0.914**	**0.834**	**0.282**	**0.335**
Ce	−0.141	**0.722**	0.196	**0.736**	**0.686**	**0.587**	**0.386**	**0.264**	**0.408**	−0.124	0.095	**0.929**	1.000	**0.966**	**0.742**	**0.303**	**0.334**
Sm	−0.164	**0.670**	0.175	**0.774**	**0.624**	**0.504**	**0.388**	0.161	**0.376**	−0.141	0.040	**0.914**	**0.966**	1.000	**0.787**	**0.301**	**0.321**
Eu	0.073	**0.391**	**0.249**	**0.605**	**0.385**	**0.302**	**0.451**	−0.019	**0.312**	−0.035	0.094	**0.834**	**0.742**	**0.787**	1.000	0.226	0.179
Pb	0.018	**0.417**	**0.338**	**0.444**	**0.528**	**0.478**	**0.544**	**0.279**	**0.473**	**0.501**	**0.365**	**0.282**	**0.303**	**0.301**	0.226	1.000	**0.343**
Ag	−0.017	**0.493**	**0.339**	**0.305**	**0.466**	**0.483**	**0.350**	**0.459**	**0.529**	0.140	**0.301**	**0.335**	**0.334**	**0.321**	0.179	**0.343**	1.000

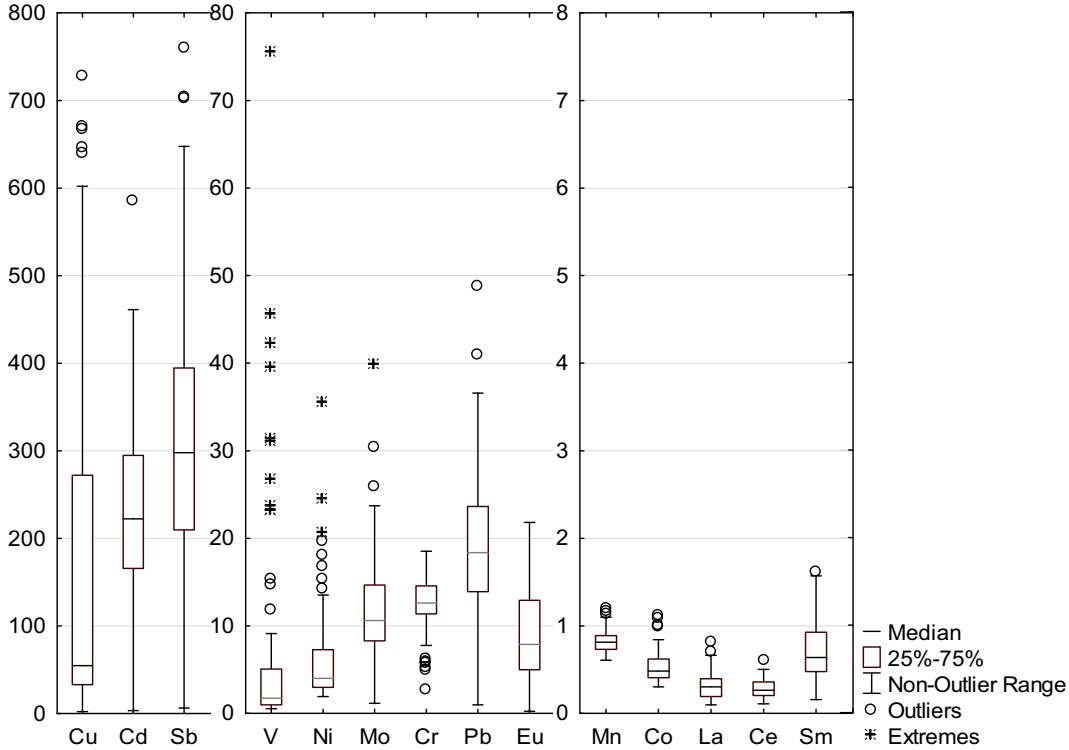

Fig. 2 Enrichment factors (EF) for all analyzed metals. EF computed considering Ti as the reference crustal component of the upper continental from Wedepohl (1995)

Table 8 Metal enrichment factors (EF) in $PM_{2.5}$. EF values have been computed, using Ti as a reference element employing upper crustal data reported by Wedepohl (1995). For seasonal median values, values in **bold** are significantly the highest ($p < 0.05$). Values in ***bold italics*** are significantly higher than one value ($p < 0.05$). Values in *italics* are significantly the lowest ($p < 0.05$)

	2013 EF					Seasonal median EF value		
	Mean	Median	Minimum	Maximum	Std. dev.	DW	R	DC
Sb	315.8	293.3	6.2	760.1	157.4	**366.7**	223.8	278.3
Cd	265.2	221.3	3.4	2116.9	257.6	257.9	215.3	221.3
Cu	203.2	59.3	2.3	1360.4	273.8	**105.2**	***55.8***	*33.1*
Pb	20.2	18.4	1.0	94.1	11.9	17.1	20.0	18.4
Cr	12.2	12.6	2.7	18.5	3.1	*11.4*	14.5	13.0
Mo	12.2	10.5	1.2	39.8	6.6	9.7	9.5	**13.2**
Eu	8.8	7.6	0.2	27.2	5.4	*5.4*	**9.3**	***9.1***
Ni	7.6	4.0	1.9	97.7	12.2	3.9	3.7	**5.3**
V	6.7	1.7	0.5	75.6	12.7	***2.3***	*1.0*	**5.5**
Mn	0.9	0.8	0.6	4.2	0.4	0.8	0.8	0.8
Sm	0.8	0.6	0.2	3.5	0.5	*0.5*	**0.9**	***0.7***
Co	0.6	0.5	0.3	3.2	0.4	0.5	0.4	0.5
La	0.4	0.3	0.1	4.1	0.5	*0.2*	**0.4**	***0.3***
Ce	0.3	0.3	0.1	3.0	0.3	*0.2*	**0.4**	***0.3***
Ag	20	0	0	225.9	45.7	0.0	0.0	0.0

Table 9 Principal component analysis. Loadings of metals in $PM_{2.5}$ related with factors

	Factor 1	Factor 2	Factor 3	Factor 4	Factor 5	Factor 6
Ti	0.468	0.123	**0.816**	0.164	0.042	0.207
V	0.054	**0.982**	0.080	0.032	0.064	0.078
Cr	0.698	0.314	0.260	− 0.003	0.122	0.388
Mn	0.348	0.137	**0.845**	0.217	0.028	0.193
Co	0.117	0.128	**0.925**	0.214	0.018	0.013
Ni	0.080	**0.937**	0.076	0.145	0.048	0.116
Cu	0.085	0.058	0.309	**0.853**	− 0.074	− 0.001
Mo	0.194	**0.866**	0.269	0.110	0.184	0.158
Cd	− 0.086	0.174	0.079	− 0.075	**0.935**	0.096
Sb	− 0.068	0.355	0.642	− 0.017	0.315	0.161
La	**0.881**	0.299	0.131	0.175	− 0.028	− 0.088
Ce	**0.934**	− 0.004	0.284	0.118	− 0.045	0.044
Sm	**0.937**	− 0.069	0.121	0.038	− 0.133	0.147
Pb	0.122	0.203	0.255	0.319	0.258	**0.746**
Ag	0.154	0.195	0.189	**0.849**	− 0.033	0.105
Eu	**0.855**	0.279	− 0.069	− 0.157	− 0.042	0.166
Eigenvalue	7.7	3.2	2.2	1.4	0.8	0.8
% Total	43.0	17.5	12.2	7.6	4.5	4.2
Cumulative	43.0	60.5	72.7	80.3	84.8	89.0

Values marked in bold are significant higher ($p<0.05$)

meteorological variations (wind conditions) between 2011 and 2013, especially during DW (Table 5), as explained in the "Source apportionment" and "Relationship between metal concentration and wind patterns" sections.

Source apportionment

Correlations and enrichment factors of metals in $PM_{2.5}$

Assigning metals to geogenic and anthropogenic sources is a complex task. Local authorities recognize anthropogenic activities as the main sources to atmospheric pollution in MCMA. Conversely, Morton-Bermea et al. (2018) identified the important influence of geogenic sources in $PM_{2.5}$ within the studied area. In the current study, Spearman's rank correlation (Table 7) led to recognize the association between $PM_{2.5}$ with V, Ni, Mo, Cd, and Sb. There is ambivalent information regarding the origin of these metals; V, Ni, and Mo have been pointed as indicators of oil fuel processes (Yuan et al. 2006; Alleman et al. 2010; Pandolfi et al. 2011), whereas, a geogenic origin of V and Ni in this area has been reported, attributed to the local host rock (Morton-Bermea et al. 2009). Thus, it could be considered that these metals come from both geogenic and anthropogenic sources. However, the mechanisms that control the impact of these sources are unclear and it will be explored in the "Source apportionment" and "Relationship between metal concentration and wind patterns" sections.

To obtain a better insight, enrichment factors (EF) have been computed, using Ti as a reference element and data from the upper crustal reported by Wedepohl (1995). Because EF values of metals are fixed by their origin, they can be used to assign elements to their geogenic or anthropogenic source. In this way, metals with $EF \approx 1$ values were assigned as unaffected by anthropogenic activities, metals with $5 < EF < 100$ as moderated enriched, and metals with $EF > 100$ as metals with a high degree of anthropogenic influence. In Fig. 2, we present EF values in box plots for all analyzed metals. Non-enriched metals (Ce, La, Co, Sm, Mn) are clearly attributed to geogenic sources; moderate enrichment metals ($EF \leq 20$ V, Ni, Mo, Cr, Pb,) are suspected to be emitted from anthropogenic activities. Cu, Cd, and Sb are strongly anthropogenic enriched, with, $EF > 100$. This is consistent with the fact that Sb has been pointed out as an emission from vehicle break wearing (Cheng

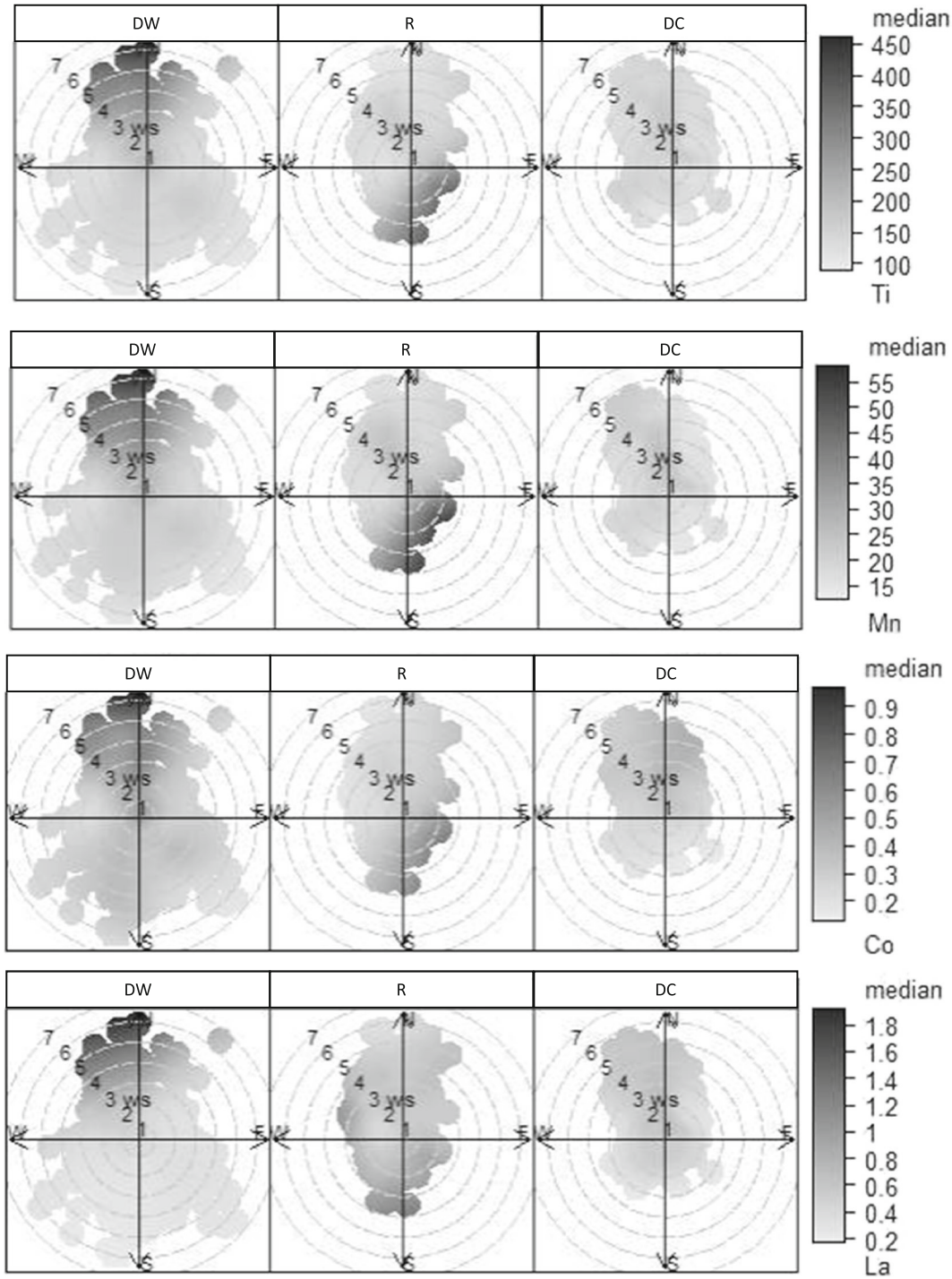

Fig. 3 Seasonally computed wind plots for metal concentrations in collected $PM_{2.5}$

et al. 2010) and that Cu and Cd are associated with industrial and metallurgic actives (Alleman et al. 2010; Zhai et al. 2014).

There is a high seasonal variability of EF values for some metals (Table 8). The significant seasonal changes of V and Ni allow us to determine that these

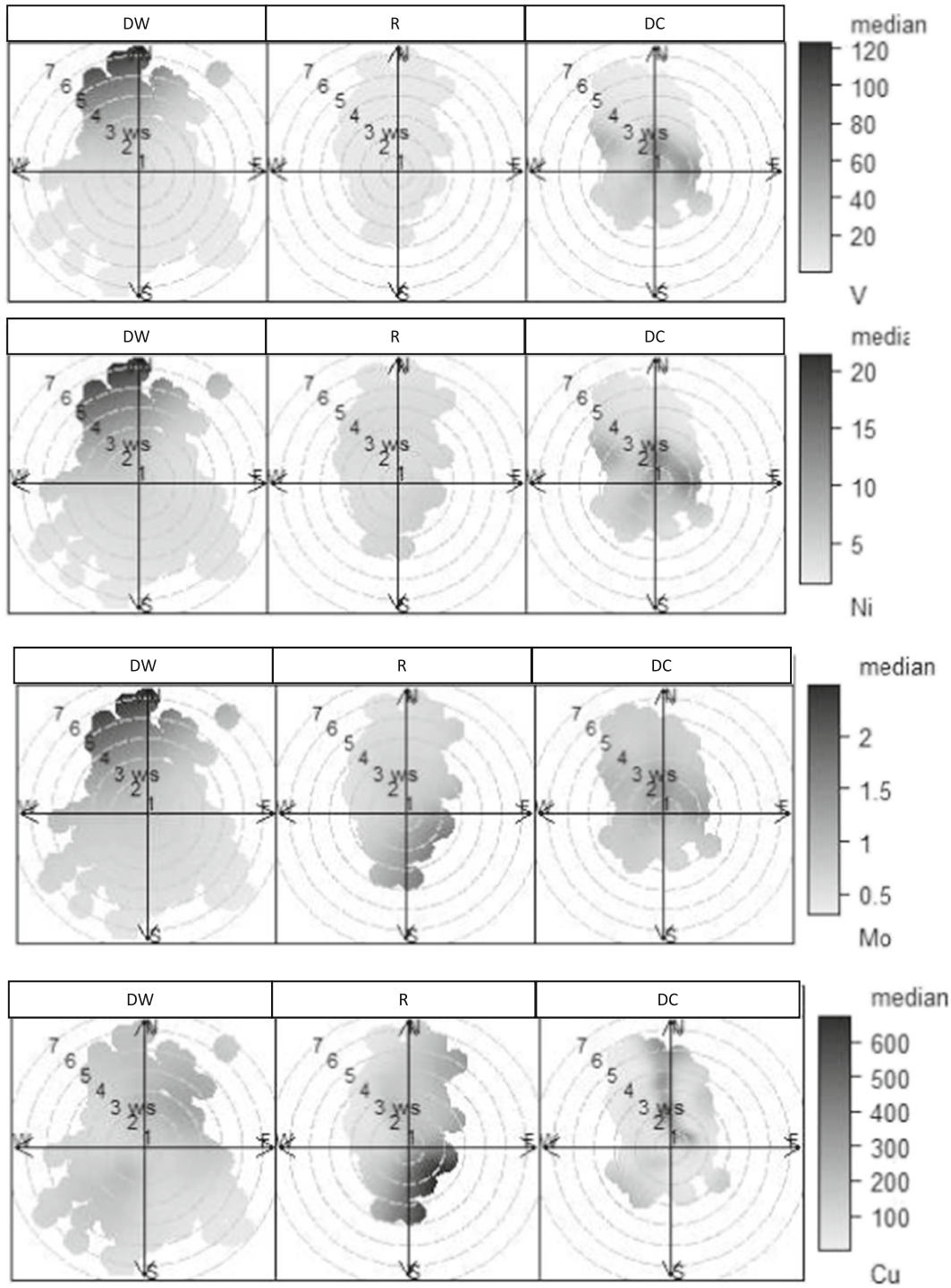

Fig. 3 (continued)

elements come from the sum of geogenic and anthropogenic sources, mixed in different relative amounts. For V, Ni, and Mo, elements correlated as shown in Table 7, and the geogenic contribution during R is evident, suggesting a decrease on the impact of anthropogenic sources during this season. Conversely, the high EF ($p < 0.05$) values during DC reveal the addition of the anthropogenic

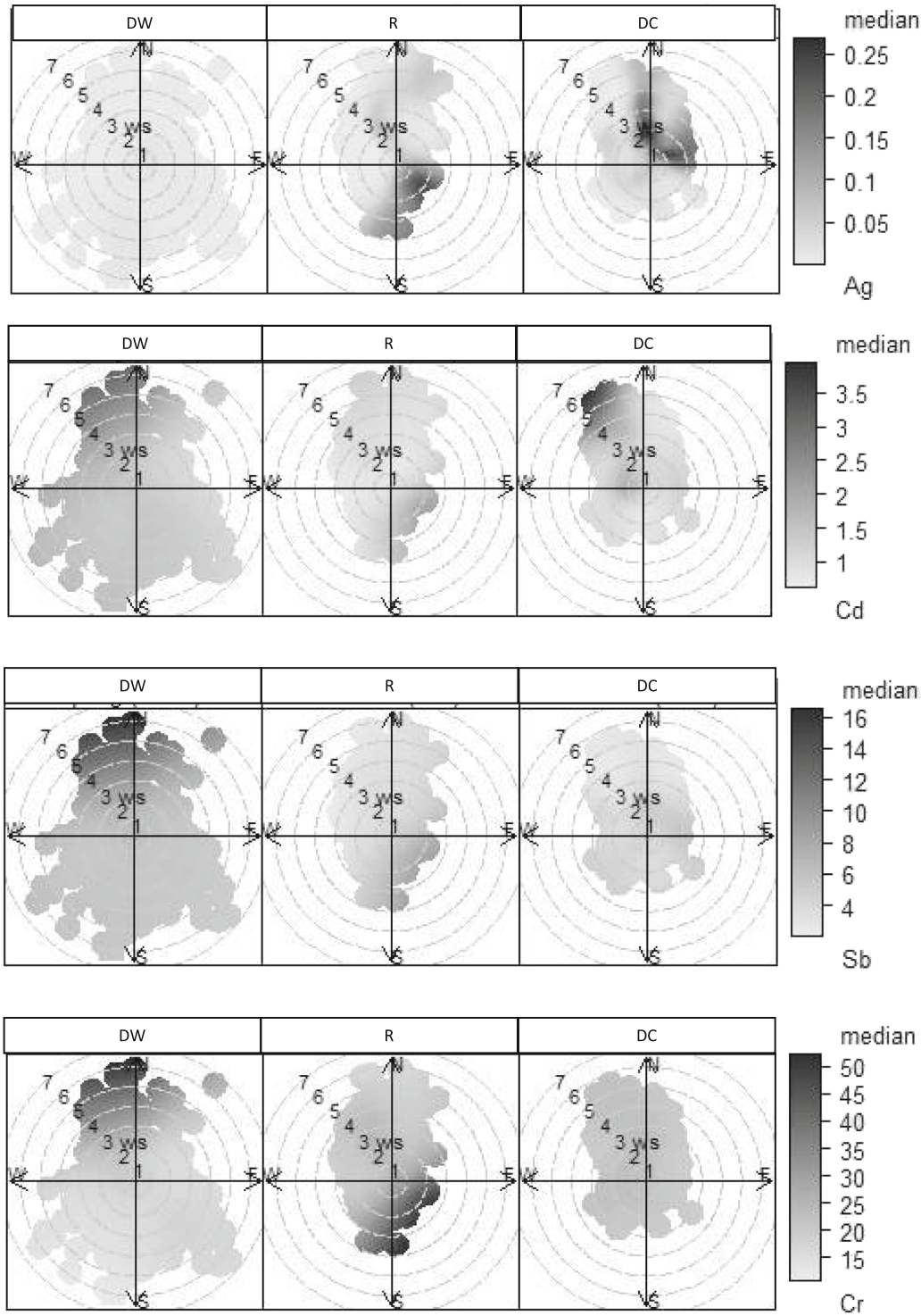

Fig. 3 (continued)

contribution. This is further supported by the Ni/V median ratio of 0.64, which is discrepant with the Ni/V ratio of samples associated with anthropogenic oil fuel combustion. Other researchers have reported Ni/V values between 2.0 and 3.5 (Yuan et al. 2006; Alleman et al. 2010; Pandolfi et al. 2011; and

Ledoux et al. 2017). Moreover, Miranda et al. 2005 found values of Ni/V ratio lower than 0.3 for the studied area, suggesting that the increase we found for this ratio may indicate an anthropogenic input.

PCA

The application of principal component analysis (PCA) (Table 9) indicated that six factors explain 89% of the total variance.

Factor 1 includes La, Sm, Eu, and Ce and explains 43.0% of total variance. This confirms the importance of geogenic sources of $PM_{2.5}$ in MCMA, as pointed by Morton-Bermea et al. 2018. It is evident that NW and NE sites presented the higher concentrations of these elements as described previously. The provenance of the geological material carrying these metals was already discussed.

Factor 2 explains 17.5% of total variance and includes Ni, V, and Mo. As previously discussed ("Correlations and enrichment factors of metals in $PM_{2.5}$" section), their origin is related to the sum of geogenic and anthropogenic sources.

Factor 3 is formed by Ti, Mn, and Co related to geogenic sources, attributed to resuspension from local soil. The percentage of total variance explained by this factor is 12.2%.

Factor 4, explaining 7.6% of total variance, involves Cu and Ag and is related to anthropogenic activities based on EF values (Table 5). This is consistent with the spatial behavior of Cu, showing that emissions of this metal are mainly located at SW and NW sites (Fig. 1), and this former characterized mainly as an industrial area, in accordance with the industrial origin of this metal (Johnson et al. 2006).

Cadmium comprises Factor 5, while Pb Factor 6. They explain 4.5% and 4.2% of total variance, respectively. These metals are attributed to anthropogenic sources related to either industrial activities or vehicular traffic.

Relationship between metal concentration and wind patterns

Wind patterns play an important role in the metal concentration variability. An assessment of wind patterns (wind flow and intensity) shows significant differences during the sampling seasons (Fig. S1). An analysis of the metal behavior by sectors, northward winds (45°–315°), eastward winds (315°–225°), southward winds (225°–135°), and westward winds (134°–45°), provides valuable information that enhances the identification of the origin of the metals as well as to the understanding of their distribution in the study area. The assessment of metal concentrations of the sectors mentioned above by means of *U* test shows that, for all sites, the concentrations of Cr, La, Sm, Ce, and Eu are significantly higher ($p < 0.05$) when southward wind occurred than those when northward winds occurred. This observation enhances the reported effects of wind patterns to some pollutants (O_3, SO_4, NO_X) described by De Foy et al. (2005); however, they observed a decrease of pollutant levels when northward wind occurred. Moreover, Cd and Sb concentrations were higher ($p < 0.05$) at all sites when northward winds occurred. This finding encloses reliable information to source identification for those metals.

A deeper analysis of metal concentration dependence on wind patterns is obtained through polar plots, computed by means of Openair package in R. This allows to analyze not only the effect of wind directions but also the effect of speed (intensity) on metal concentrations. In Fig. 3, polar plots are presented seasonally for the analyzed metals. The wind patterns used to be light wind (US Weather Bureau description) with an average speed of 2.3 m s^{-1} (Fig. S1). However, the impact assessment of strong wind episodes exceeding 5 m s^{-1}, recorded during the afternoon on April 10, April 16, May 4, and August 2 at NW, NE, and SE provides interesting information. The maximum concentrations for Ti, Mn, Co, La, Eu, Sm, and Ce occurred during these episodes. The above provides evidence suggesting that wind intensity is responsible for carrying geogenic material, in spite of wind direction.

On the other hand, during DC, there were conditions of atmospheric stability with calm winds and low temperature, which resulted in an accumulation of metals from local sources. It was also possible to identify that during this season, the highest concentrations of V, Ni, and Mo occurred when the wind blew from the SE, suggesting that the corresponding anthropogenic component of these metals can be

differentiated only during DC. These statements highlight the importance of meteorological conditions to the impact and distribution of metals in $PM_{2.5}$ in MCMA.

Conclusion

According to previous information of metals contained in $PM_{2.5}$ in the atmospheric environment of the MCMA, the geochemical data generated in this study were used to verify previous information of the metal concentration ranges and their spatial and temporal behavior as well as to recognize the sources of emission in the area. Furthermore, the use of statistical tools to the geochemical and meteorological data highlighted the importance of wind intensity to the impact of emission sources.

The 17% increase in $PM_{2.5}$ mass concentrations observed from 2011 to 2013 is attributable to differences in the impact of geogenic sources. This is consistent with changes in wind intensity. The mechanism by which the geogenic sources have been highly impacted was revealed by means of wind plots. This allowed us to conclude that high-speed episodes (5 m s^{-1}) are responsible for raising geogenic metal concentrations rather than wind direction. Despite these differences in metal concentrations, the spatial distribution is consistent with the 2011 observations.

The identification of the emission sources was inferred from the information obtained from EF and PCA. The seasonal evaluation of EF revealed changes in the behavior of the ratios of geogenic and anthropogenic sources for metals associated to mixed sources (Ni and V), as a consequence of meteorological changes during DC season.

Improved metal concentration analysis, identification of source emissions, and distribution patterns in $PM_{2.5}$ may result in the development of reliable public policies, based on the potential risk of toxicological effects of breathable particulate matter since the MCMA houses more than 20 million inhabitants.

Funding information This study was performed with the financial support of Project IN103717 from DGAPA (Dirección General de Personal Académico, UNAM). Rodrigo Garza-Galindo gratefully acknowledges a grant from CONACyT (Consejo Nacional de Ciencia y Tecnología).

References

Aldabe, J., Elustondo, D., Santamaría, C., Lasheras, E., Pandolfi, M., Alastuey, A., Querol, X., & Santamaría, J. M. (2011). Chemical characterisation and source apportionment of PM2. 5 and PM10 at rural, urban and traffic sites in Navarra (north of Spain). *Atmospheric Research, 102*(1), 191–205.

Alleman, L. Y., Lamaison, L., Perdrix, E., Robache, A., & Galloo, J. C. (2010). PM 10 metal concentrations and source identification using positive matrix factorization and wind sectoring in a French industrial zone. *Atmospheric Research, 96*(4), 612–625.

Amador-Muñoz, O., Villalobos-Pietrini, R., Miranda, J., & Vera-Avila, L. E. (2011). Organic compounds of PM 2.5 in Mexico Valley: spatial and temporal patterns, behavior and sources. *Science of the Total Environment, 409*(8), 1453–1465.

Amador-Muñoz, O., Bazán-Torija, S., Villa-Ferreira, S. A., Villalobos-Pietrini, R., Bravo-Cabrera, J. L., Munive-Colín, Z., Hernández-Mena, L., Saldarriaga-Noreña, H., & Murillo-Tovar, M. A. (2013). Opposing seasonal trends for polycyclic aromatic hydrocarbons and PM_{10}, health risk and sources in Southwest Mexico City. *Atmospheric Research., 122*, 199–212.

Barrera, V. A., Miranda, J., Espinosa, A. A., Meinguer, J., Martínez, J. N., Cerón, E., et al. (2012). Contribution of soil, sulfate, and biomass burning sources to the elemental composition of PM10 from Mexico city. *International Journal of Environmental Research, 6*(3), 597–612.

Cheng, Y., Lee, S. C., Ho, K. F., Chow, J. C., Watson, J. G., Louie, P. K. K., Cao, J. J., & Hai, X. (2010). Chemically-speciated on-road PM2. 5 motor vehicle emission factors in Hong Kong. *Science of the Total Environment, 408*(7), 1621–1627.

DeCarlo, P. F., Dunlea, E. J., Kimmel, J. R., Aiken, A. C., Sueper, D., Crounse, J., Wennberg, P. O., Emmons, L., Shinozuka, Y., Clarke, A., Zhou, J., Tomlinson, J., Collins, D. R., Knapp, D., Weinheimer, A. J., Montzka, D. D., Campos, T., & Jimenez, J. L. (2008). Fast airborne aerosol size and chemistry measurements above Mexico City and Central Mexico during the MILAGRO campaign. *Atmospheric Chemistry and Physics, 8*(14), 4027–4048.

De Foy, B., Caetano, E., Magana, V., Zitácuaro, A., Cárdenas, B., Retama, A., et al. (2005). Mexico City basin wind circulation during the MCMA-2003 field campaign. *Atmospheric Chemistry and Physics Discussions, 5*(3), 2503–2558.

Dongarrà, G., Manno, E., Varrica, D., Lombardo, M., & Vultaggio, M. (2010). Study on ambient concentrations of PM 10, PM 10–2.5, PM 2.5 and gaseous pollutants. Trace elements and chemical speciation of atmospheric particulates. *Atmospheric Environment, 44*(39), 5244–5257.

Hays, M. D., Cho, S. H., Baldauf, R., Schauer, J. J., & Shafer, M. (2011). Particle size distributions of metal and non-metal elements in an urban near-highway environment. *Atmospheric Environment, 45*(4), 925–934.

Hernández-López, A. E., Miranda, J., & Pineda, J. C. (2016). X-ray fluorescence analysis of fine atmospheric aerosols from a site in Mexico City. *Journal of Nuclear. Physics, Material Sciences, Radiation and Applications., 4*(1), 25–30.

Johnson, K. S., Foy, B. D., Zuberi, B., Molina, L. T., Molina, M. J., Xie, Y., et al. (2006). Aerosol composition and source apportionment in the Mexico City Metropolitan Area with

PIXE/PESA/STIM and multivariate analysis. *Atmospheric Chemistry and Physics, 6*(12), 4591–4600.

Kampa, M., & Castanas, E. (2008). Human health effects of air pollution. *Environmental Pollution, 151*(2), 362–367.

Kulshrestha, A., Satsangi, P. G., Masih, J., & Taneja, A. (2009). Metal concentration of PM2. 5 and PM10 particles and seasonal variations in urban and rural environment of Agra, India. *Science of the Total Environment, 407*(24), 6196–6204.

Ledoux, F., Kfoury, A., Delmaire, G., Roussel, G., El Zein, A., & Courcot, D. (2017). Contributions of local and regional anthropogenic sources of metals in PM2.5 at an urban site in northern France. *Chemosphere, 181*, 713–724.

Michael, S., Montag, M., & Dott, W. (2013). Pro-inflammatory effects and oxidative stress in lung macrophages and epithelial cells induced by ambient particulate matter. *Environmental Pollution, 183*, 19–29.

Miranda, J., Barrera, V. A., Espinosa, A. A., Galindo, O. S., & Meinguer, J. (2005). PIXE analysis of atmospheric aerosols in Mexico City. *X-Ray Spectrometry, 34*(4), 315–319.

Molina, L. T., Madronich, S., Gaffney, J. S., Apel, E., de Foy, B., Fast, J., Ferrare, R., Herndon, S., Jimenez, J. L., Lamb, B., Osornio-Vargas, A. R., Russell, P., Schauer, J. J., Stevens, P. S., Volkamer, R., & Zavala, M. (2010). An overview of the MILAGRO 2006 campaign: Mexico City emissions and their transport and transformation. *Atmospheric Chemistry and Physics, 10*, 8697–8760.

Moreno, T., Querol, X., Alastuey, A., Reche, C., Cusack, M., Amato, F., Pandolfi, M., Pey, J., Richard, A., Prévôt, A. S. H., Furger, M., & Gibbons, W. (2011). Variations in time and space of trace metal aerosol concentrations in urban areas and their surroundings. *Atmospheric Chemistry and Physics, 11*(17), 9415–9430.

Morton-Bermea, O., Hernández-Álvarez, E., González-Hernández, G., Romero, F., Lozano, R., & Beramendi-Orosco, L. E. (2009). Assessment of heavy metal pollution in urban topsoils from the metropolitan area of Mexico City. *Journal of Geochemical Exploration, 101*(3), 218–224.

Morton-Bermea, O., Amador-Muñoz, O., Martínez-Trejo, L., Hernández-Alvarez, E., Beramendi-Orosco, L., & García-Arreola, M. E. (2014). Platinum in $PM_{2.5}$ of the metropolitan area of Mexico City. *Environmental Geochemical Health, 36*, 987–994.

Morton-Bermea, O., Garza-Galindo, R., Hernández-Álvarez, E., Amador-Muñoz, O., Garcia-Arreola, M. E., Ordoñez-Godínez, S. L., Beramendi-Orosco, L., Santos-Medina, G. L., Miranda, J., & Rosas-Pérez, I. (2018). Recognition of the importance of geogenic sources in the content of metals in PM 2.5 collected in the Mexico City Metropolitan Area. *Environmental Monitoring and Assessment, 190*(2), 83.

Mugica, V., Ortiz, E., Molina, L., De Vizcaya-Ruiz, A., Nebot, A., Quintana, R., et al. (2009). PM composition and source reconciliation in Mexico City. *Atmospheric Environment, 43*(32), 5068–5074.

Pandolfi, M., Gonzalez-Castanedo, Y., Alastuey, A., Jesus, D., Mantilla, E., de la Campa, A. S., et al. (2011). Source apportionment of PM 10 and PM 2.5 at multiple sites in the strait of Gibraltar by PMF: impact of shipping emissions. *Environmental Science and Pollution Research, 18*(2), 260–269.

Perrone, M. G., Gualtieri, M., Consonni, V., Ferrero, L., Sangiorgi, G., Longhin, E., Ballabio, D., Bolzacchini, E., & Camatini, M. (2013). Particle size, chemical composition, seasons of the year and urban, rural or remote site origins as determinants of biological effects of particulate matter on pulmonary cells. *Environmental Pollution, 176*, 215–227.

Querol, X., Pey, J., Minguillón, M. C., Pérez, N., Alastuey, A., Viana, M., Moreno, T., Bernabé, R. M., Blanco, S., Cárdenas, B., Vega, E., Sosa, G., Escalona, S., Ruiz, H., & Artíñano, B. (2008). PM speciation and sources in Mexico during the MILAGRO-2006 campaign. *Atmospheric Chemistry and Physics, 8*(1), 111–128.

Saliba, N. A., El Jam, F., El Tayar, G., Obeid, W., & Roumie, M. (2010). Origin and variability of particulate matter (PM10 and PM2. 5) mass concentrations over an Eastern Mediterranean city. *Atmospheric Research, 97*(1–2), 106–114.

Santibáñez-Andrade, M., Quezada-Maldonado, E. M., Osornio-Vargas, Á., Sánchez-Pérez, Y., & García-Cuellar, C. M. (2017). Air pollution and genomic instability: the role of particulate matter in lung carcinogenesis. *Environmental Pollution, 229*, 412–422.

Stone, E. A., Snyder, D. C., Sheesley, R. J., Sullivan, A. P., Weber, R. J., & Schauer, J. J. (2008). Source apportionment of fine organic aerosol in Mexico City during the MILAGRO experiment 2006. *Atmospheric Chemistry and Physics, 8*(5), 1249–1259.

Uria-Tellaetxe, I., & Carslaw, D. C. (2014). Conditional bivariate probability function for source identification. *Environmental Modelling & Software, 59*, 1–9.

Wang, Q., Kobayashi, K., Lu, S., Nakajima, D., Wang, W., Zhang, W., Sekiguchi, K., & Terasaki, M. (2016). Studies on size distribution and health risk of 37 species of polycyclic aromatic hydrocarbons associated with fine particulate matter collected in the atmosphere of a suburban area of Shanghai city, China. *Environmental Pollution, 214*, 149–160.

Warneck, P., & Williams, J. (2012). *The atmospheric Chemist's companion: numerical data for use in the atmospheric sciences*. Springer Science & Business Media.

Wedepohl, K. H. (1995). The composition of the continental crust. *Geochimica et Cosmochimica Acta, 59*(7), 1217–1232.

World Health Organization. (2016). *Ambient air pollution: A global assessment of exposure and burden of disease*

Yuan, Z., Lau, A. K. H., Zhang, H., Yu, J. Z., Louie, P. K., & Fung, J. C. (2006). Identification and spatiotemporal variations of dominant PM 10 sources over Hong Kong. *Atmospheric Environment, 40*(10), 1803–1815.

Zhang, C., Ni, Z., & Ni, L. (2015). Multifractal detrended cross-correlation analysis between PM2. 5 and meteorological factors. *Physica A: Statistical Mechanics and its Applications, 438*, 114–123.

Zhai, Y., Liu, X., Chen, H., Xu, B., Zhu, L., Li, C., & Zeng, G. (2014). Source identification and potential ecological risk assessment of heavy metals in PM2. 5 from Changsha. *Science of the Total Environment, 493*, 109–115.